

An Error Control Framework for Computing the Exponential of Matrices Arising from the Finite Element Discretization

Fuminori Tatsuoka^{1*}, Yuto Miyatake² and Tomohiro Sogabe³

^{1*}Corporate Research and Development Division, IHI Corporation, 1 Shin-Nakahara-cho, Isogo-ku, Yokohama, 235-8501, Kanagawa, Japan.

²D3 Center, The University of Osaka, 1-32 Machikaneyama-cho, Toyonaka, 560-0043, Osaka, Japan.

³Graduate School of Engineering, Nagoya University, Furo-cho, Chikusa, 464-8603, Nagoya, Japan.

*Corresponding author(s). E-mail(s): tatsuoka3229@ihi-g.com;
Contributing authors: yuto.miyatake.cmc@osaka-u.ac.jp;
sogabe@na.nuap.nagoya-u.ac.jp;

Abstract

Several methods for computing the action of the matrix exponential $e^{\mathbf{A}\mathbf{b}}$ are expressed by substituting \mathbf{A} into a rational approximation of the scalar exponential function. The error of such methods can be estimated using the numerical range of \mathbf{A} , which enables the computation of $e^{\mathbf{A}\mathbf{b}}$ with a prescribed accuracy. However, when the input matrix has the structure $\mathbf{A} = \tau\mathbf{M}^{-1}\mathbf{K}$, this approach is challenging because computing the bounding box of numerical range is difficult and the numerical range may be too large to construct rational approximations on it. In this paper, focusing on the case where \mathbf{M} is a well-conditioned symmetric positive definite matrix, we propose considering the numerical range of a similarity transformed matrix of \mathbf{A} . The numerical range of transformed matrix is not only numerically computable but can also be theoretically bounded depending on properties of \mathbf{K} . Numerical experiments confirm that the computations can be performed within the prescribed error tolerance.

Keywords: matrix function, matrix exponential, rational approximation, numerical range

MSC Classification: 65F60 , 15A16

1 Introduction

For a square matrix $\mathbf{A} \in \mathbb{C}^{n \times n}$, its exponential is defined as [1, Eq. (10.1)]

$$e^{\mathbf{A}} := \mathbf{I} + \mathbf{A} + \frac{1}{2!}\mathbf{A}^2 + \frac{1}{3!}\mathbf{A}^3 + \dots . \quad (1)$$

The matrix exponential allows us to represent the solutions of linear initial value problems: for the initial value problem

$$\dot{\mathbf{u}}(t) = \mathbf{A}\mathbf{u}(t), \quad \mathbf{u}(0) = \mathbf{u}_0, \quad (2)$$

it holds that

$$\mathbf{u}(t) = e^{t\mathbf{A}}\mathbf{u}_0. \quad (3)$$

This relation facilitates the construction of numerical solvers called exponential integrators for problems that are challenging to solve with conventional methods such as Runge–Kutta methods; see e.g. [2] for more details. Hence, computational methods for $e^{\mathbf{A}}\mathbf{b}$ ($\mathbf{b} \in \mathbb{C}^n$), are of significant importance in numerical analysis.

Roughly speaking, computational methods for $e^{\mathbf{A}}\mathbf{b}$ can be classified into two categories. The first category includes methods that substitute \mathbf{A} into a prescribed scalar rational approximation $r(z) \approx e^z$, such as the truncated Taylor series [3],

$$e^{\mathbf{A}}\mathbf{b} \approx \left(\mathbf{I} + \mathbf{A} + \frac{1}{2!}\mathbf{A}^2 + \frac{1}{3!}\mathbf{A}^3 + \dots + \frac{1}{m!}\mathbf{A}^m \right) \mathbf{b}. \quad (4)$$

sub-diagonal Padé approximation [4], polynomial interpolation [5, 6], and numerical quadrature [7–9]. The other category includes methods based on projection on an appropriate low dimensional subspace. Let $\mathbf{V} \in \mathbb{C}^{n \times m}$ ($m \ll n$) be an orthogonal basis of a certain subspace. Then, $e^{\mathbf{A}}\mathbf{b}$ is approximated by $\mathbf{V}e^{\mathbf{H}}\mathbf{V}^*\mathbf{b}$, where $\mathbf{H} = \mathbf{V}^*\mathbf{A}\mathbf{V} \in \mathbb{C}^{m \times m}$. To construct \mathbf{V} , polynomial Krylov subspace, extended Krylov subspace, and rational Krylov subspace have been used [10–12].

While methods in the latter category are often employed due to their efficiency in the context of exponential integrators, methods in the former category remain important for several reasons. For example, some of these methods are applicable even in limited-memory environments, i.e., when n is so large that storing the block matrix $\mathbf{V} \in \mathbb{C}^{n \times m}$ with moderate m becomes prohibitive. For another reason, when $r(z)$ is given in partial fraction form (e.g., the subdiagonal Padé approximation and quadrature-based algorithms), the resulting algorithm is well-suited for parallel computing.

In this paper, we focus on the methods based on the first category, i.e., those based on scalar rational approximations. To guarantee the approximation accuracy, it is important to check $\|r(\mathbf{A}) - e^{\mathbf{A}}\|_2 \leq \epsilon$ for a given tolerance ϵ . A straightforward approach to bound $\|r(\mathbf{A}) - e^{\mathbf{A}}\|_2$ is to utilize the numerical range (also called the field of values) of \mathbf{A} : $\mathcal{W}(\mathbf{A}) := \{\mathbf{v}^*\mathbf{A}\mathbf{v} : \mathbf{v} \in \mathbb{C}^n, \|\mathbf{v}\|_2 = 1\}$. It is known that $\mathcal{W}(\mathbf{A})$ is a

$(1 + \sqrt{2})$ -spectral set for \mathbf{A} (see [13]), and therefore, for any rational function r that is bounded on $\mathcal{W}(\mathbf{A})$, it holds that

$$\|r(\mathbf{A}) - e^{\mathbf{A}}\|_2 \leq (1 + \sqrt{2}) \sup_{z \in \mathcal{W}(\mathbf{A})} |r(z) - e^z|. \quad (5)$$

While the numerical range $\mathcal{W}(\mathbf{A})$ cannot be obtained analytically and estimating it precisely is computationally expensive, a rectangular region \mathcal{R} that contains $\mathcal{W}(\mathbf{A})$ can be obtained with cheaper costs. Specifically, the left and right endpoints of \mathcal{R} are given by the extreme eigenvalues of $(\mathbf{A} + \mathbf{A}^*)/2$, and the top and bottom endpoints correspond to the extreme eigenvalues of $(\mathbf{A} - \mathbf{A}^*)/2i$. This fact is noted in e.g. [6] and a special case of the algorithm estimating $\mathcal{W}(\mathbf{A})$ in [14].

Based on the above discussion, an error control framework for $e^{\mathbf{A}}\mathbf{b}$ using $r(z)$ can be obtained as in Algorithm 1. In this framework, we first determine \mathcal{R} enclosing $\mathcal{W}(\mathbf{A})$ by computing the extreme eigenvalues of the Hermitian and skew Hermitian parts of \mathbf{A} . We then construct $r(z) \approx e^z$ on \mathcal{R} such that the condition $\|r(\mathbf{A}) - e^{\mathbf{A}}\|_2 \leq \epsilon$ is satisfied. A similar strategy had been proposed to provide an error bound of polynomial interpolation [5]¹.

Algorithm 1 An error control framework based on numerical range for $e^{\mathbf{A}}\mathbf{b}$.

Input $\mathbf{A}, \mathbf{b}, \epsilon$

- 1: Compute the maximum (minimum) eigenvalue μ_{\max} (μ_{\min}) of $(\mathbf{A} + \mathbf{A}^*)/2$
- 2: Compute the maximum (minimum) eigenvalue ν_{\max} (ν_{\min}) of $(\mathbf{A} - \mathbf{A}^*)/2i$
- 3: $\mathcal{R} = \{z \in \mathbb{C}: \text{Re}(z) \in [\mu_{\max}, \mu_{\min}], \text{Im}(z) \in [\nu_{\max}, \nu_{\min}]\} \quad (\supseteq \mathcal{W}(\mathbf{A}))$
- 4: Construct a rational approximation $r(z) \approx e^z$ on \mathcal{R} such that

$$\max_{z \in \mathcal{R}} |r(z) - e^z| \leq \frac{\epsilon}{1 + \sqrt{2}}. \quad (6)$$

Output $r(\mathbf{A})\mathbf{b} \quad (\|r(\mathbf{A})\mathbf{b} - e^{\mathbf{A}}\mathbf{b}\|_2 \leq \epsilon \|\mathbf{b}\|_2)$

In this study, we focus on the situation $\mathbf{A} = \tau \mathbf{M}^{-1} \mathbf{K}$, where $\tau > 0$, $\mathbf{M} \in \mathbb{R}^{n \times n}$ is a well-conditioned symmetric positive definite (SPD) matrix, and $\mathbf{K} \in \mathbb{R}^{n \times n}$. For example, such matrices arise from the finite element discretization of advection-diffusion equations. However, there are two difficulties to apply Algorithm 1 to this situation. First, to the best of our knowledge, there are no estimates and computational methods for obtaining eigenvalues of (skew) symmetric part of $\mathbf{A} = \tau \mathbf{M}^{-1} \mathbf{K}$, and therefore computing the rectangle region \mathcal{R} is not straightforward. Second, $\mathcal{W}(\mathbf{A})$ can be so large that an accurate rational approximation cannot be constructed on it. For example, the left figure in Figure 1 illustrates $\mathcal{W}(\mathbf{A})$ for a test matrix from an advection-diffusion equation described in Section 3. The figure shows that $\mathcal{W}(\mathbf{A})$ extends into the right half plane. For this case, $r(z)$ must deal with large values (e.g., $e^{17.29}$) with the error tolerance ϵ , which is practically impossible.

¹Although ϕ -function $(e^z - 1)/z$ is focused in [5] rather than exponential function, the method described therein remains applicable to exponential, see [6].

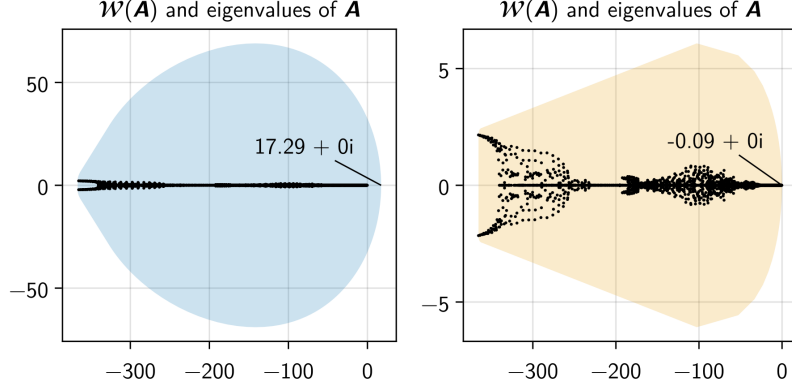


Fig. 1 Comparison of $\mathcal{W}(\mathbf{A})$ and $\mathcal{W}(\hat{\mathbf{A}})$. The matrix \mathbf{A} is a test matrix described in Section 3.1, obtained by discretizing the two dimensional advection–diffusion equation on a square domain with a P2 finite element method. The set $\mathcal{W}(\hat{\mathbf{A}})$ lies in the left half plane.

In this paper, to apply the error control framework (Algorithm 1) to $\mathbf{A} = \tau \mathbf{M}^{-1} \mathbf{K}$, we propose to use $\mathcal{W}(\hat{\mathbf{A}})$ instead of $\mathcal{W}(\mathbf{A})$, where $\hat{\mathbf{A}} := \mathbf{M}^{1/2} \mathbf{A} \mathbf{M}^{-1/2}$. There are three convenient properties for $\mathcal{W}(\hat{\mathbf{A}})$. First, $\mathcal{W}(\hat{\mathbf{A}})$ also provide us with an upper bound on $\|r(\mathbf{A}) - e^{\mathbf{A}}\|_2$ that is a value proportional to the supremum of $|r(z) - e^z|$ over $\mathcal{W}(\hat{\mathbf{A}})$. Second, a rectangular region enclosing $\mathcal{W}(\hat{\mathbf{A}})$ can be obtained numerically by solving typical generalized eigenvalue problems. Third, if $\mathcal{W}(\mathbf{K})$ lies in the left half plane, then $\mathcal{W}(\hat{\mathbf{A}})$ still lies in the left half plane. The third property can be seen in the right figure in Fig. 1. Based on them, we establish an error control framework for computing $e^{\tau \mathbf{M}^{-1} \mathbf{K} \mathbf{b}}$.

The organization of this paper is as follows. Section 2 presents the error control framework for $\mathbf{A} = \tau \mathbf{M}^{-1} \mathbf{K}$. Section 3 provides numerical results, and Section 4 concludes this paper.

2 Error control framework for $\mathbf{A} = \tau \mathbf{M}^{-1} \mathbf{K}$

In this section, we show some properties of $\mathcal{W}(\hat{\mathbf{A}})$ and propose the error control framework. Firstly, it is shown that $\mathcal{W}(\hat{\mathbf{A}})$ gives us an upper bound on the error $r(\mathbf{A}) - e^{\mathbf{A}}$ as follows:

Theorem 1 For $\mathbf{A} = \tau \mathbf{M}^{-1} \mathbf{K}$, where $\tau > 0$, $\mathbf{M} \in \mathbb{R}^{n \times n}$ is an SPD matrix, and $\mathbf{K} \in \mathbb{R}^{n \times n}$, define $\hat{\mathbf{A}} = \mathbf{M}^{1/2} \mathbf{A} \mathbf{M}^{-1/2}$. Then, for any rational function $r(z)$ that is bounded on $\mathcal{W}(\hat{\mathbf{A}})$, it follows that

$$\|r(\mathbf{A}) - e^{\mathbf{A}}\|_2 \leq (1 + \sqrt{2}) \kappa(\mathbf{M})^{1/2} \sup_{z \in \mathcal{W}(\hat{\mathbf{A}})} |r(z) - e^z|, \quad (7)$$

where $\kappa(\mathbf{M}) = \|\mathbf{M}\|_2 \|\mathbf{M}^{-1}\|_2$.

Proof For notational simplicity we write $g(\mathbf{A}) = r(\mathbf{A}) - e^{\mathbf{A}}$. Using the property in [1, Thm. 1.13 (c)], we can rewrite $g(\mathbf{A})$ as

$$g(\mathbf{A}) = g(\mathbf{M}^{-1/2} \mathbf{M}^{1/2} \mathbf{A} \mathbf{M}^{-1/2} \mathbf{M}^{1/2}) = \mathbf{M}^{-1/2} g(\mathbf{M}^{1/2} \mathbf{A} \mathbf{M}^{-1/2}) \mathbf{M}^{1/2} = \mathbf{M}^{-1/2} g(\hat{\mathbf{A}}) \mathbf{M}^{1/2}. \quad (8)$$

Thus, we have

$$\|g(\mathbf{A})\|_2 = \|\mathbf{M}^{-1/2} g(\hat{\mathbf{A}}) \mathbf{M}^{1/2}\|_2 \leq \kappa(\mathbf{M}^{1/2}) \|g(\hat{\mathbf{A}})\|_2 \quad (9)$$

because $\kappa(\mathbf{M}^{1/2}) = \kappa(\mathbf{M})^{1/2}$. By using (5) with the matrix $\hat{\mathbf{A}}$, we have (7). \square

Remark 1 Because the eigenvalues of $\hat{\mathbf{A}}$ coincide with that of \mathbf{A} , $\mathcal{W}(\hat{\mathbf{A}})$ is $(1 + \sqrt{2})\kappa(\mathbf{A})$ -spectral set of \mathbf{A} . See, e.g., [13] for the definition of spectral sets.

Next, we show that a rectangle region enclosing $\mathcal{W}(\hat{\mathbf{A}})$ can be obtained by solving generalized eigenvalue problems as follows:

Proposition 2 *Let us define*

$$\mathbf{D} := \frac{1}{2}(\mathbf{K} + \mathbf{K}^\top), \quad \mathbf{C} := \frac{1}{2i}(\mathbf{K} - \mathbf{K}^\top). \quad (10)$$

Then, the left (right) endpoint of $\mathcal{W}(\hat{\mathbf{A}})$ is the minimum (maximum) eigenvalue of the generalized eigenvalue problem $(\tau\mathbf{D})\mathbf{x} = \lambda\mathbf{M}\mathbf{x}$. Similarly the top (bottom) endpoint of $\mathcal{W}(\hat{\mathbf{A}})$ is the maximum (minimum) eigenvalue of the generalized eigenvalue problem $(\tau\mathbf{C})\mathbf{x} = \lambda\mathbf{M}\mathbf{x}$.

Proof For $\hat{\mathbf{A}} = \mathbf{M}^{1/2} \mathbf{A} \mathbf{M}^{-1/2} = \tau \mathbf{M}^{-1/2} \mathbf{K} \mathbf{M}^{-1/2}$, its symmetric and skew-symmetric part are $\tau \mathbf{M}^{-1/2} \mathbf{D} \mathbf{M}^{-1/2}$ and $\tau \mathbf{M}^{-1/2} \mathbf{C} \mathbf{M}^{-1/2}$, respectively because \mathbf{M} is SPD. Therefore, the eigenvalues of the symmetric parts coincide with those of $\mathbf{M}^{-1}(\tau\mathbf{D})$, and the eigenvalues of the skew-symmetric part coincide with those of $\mathbf{M}^{-1}(\tau\mathbf{C})$. \square

It is known that the numerical range of the advection-diffusion operator lies in the left half plane. In addition, if the finite element method is employed, the numerical range of the resulting matrix \mathbf{K} also lies in the left half plane [15]. The set $\mathcal{W}(\hat{\mathbf{A}})$ inherits this convenient property as follows:

Proposition 3 *Suppose that $\mathcal{W}(\mathbf{K})$ is in the left half plane. Then, $\mathcal{W}(\hat{\mathbf{A}})$ is also in the left half plane.*

Proof For $\mathbf{v} \in \mathbb{C}^n$, we have

$$\operatorname{Re}(\mathbf{v}^* \hat{\mathbf{A}} \mathbf{v}) = \operatorname{Re}(\tau \mathbf{v}^* \mathbf{M}^{-1/2} \mathbf{K} \mathbf{M}^{-1/2} \mathbf{v}) = \tau \operatorname{Re} \left((\mathbf{M}^{-1/2} \mathbf{v})^* \mathbf{K} (\mathbf{M}^{-1/2} \mathbf{v}) \right) \leq 0. \quad (11)$$

\square

At the end of this section, we summarize the error-control framework in Algorithm 2. First, we determine a rectangle \mathcal{R} enclosing $\mathcal{W}(\hat{\mathbf{A}})$ by computing the extreme eigenvalues of $(\tau\mathbf{D}, \mathbf{M})$ and $(\tau\mathbf{C}, \mathbf{M})$, respectively. Then, following a procedure similar to Algorithm 2, we construct a rational function $r(z) \approx e^z$ on \mathcal{R} and compute $r(\mathbf{A})\mathbf{b}$. Note that the eigenvalues and the condition number required in Algorithm 2 only need to be estimated roughly. For example, it suffices to obtain a lower bound for $\kappa(\mathbf{M})$. If $\kappa(\mathbf{M})$ is computed with a relative error bounded by δ (< 1), yielding an approximate value $\tilde{\kappa}$, one can use $\tilde{\kappa}/(1 - \delta)$ in place of $\kappa(\mathbf{M})$ because the inequality $\kappa(\mathbf{M}) \geq \tilde{\kappa}/(1 - \delta)$ holds.

Algorithm 2 The proposed error control framework for $e^{\mathbf{A}}\mathbf{b}$ with $\mathbf{A} = \tau\mathbf{M}^{-1}\mathbf{K}$

Input $\tau, \mathbf{M}, \mathbf{K}, \mathbf{b}, \epsilon$

- 1: $\mathbf{D} = (\mathbf{K} + \mathbf{K}^\top)/2, \quad \mathbf{C} = (\mathbf{K} - \mathbf{K}^\top)/2i$
- 2: Compute the maximum (minimum) eigenvalue μ_{\max} (μ_{\min}) of the generalized eigenvalue problem $(\tau\mathbf{D})\mathbf{x} = \mu\mathbf{M}\mathbf{x}$.
- 3: Compute the maximum (minimum) eigenvalue ν_{\max} (ν_{\min}) of the generalized eigenvalue problem $(\tau\mathbf{C})\mathbf{x} = \mu\mathbf{M}\mathbf{x}$.
- 4: $\mathcal{R} = \{z \in \mathbb{C} : \text{Re}(z) \in [\mu_{\min}, \mu_{\max}], \text{Im}(z) \in [\nu_{\min}, \nu_{\max}]\}$ ($\supseteq \mathcal{W}(\hat{\mathbf{A}})$)
- 5: Compute $\kappa(\mathbf{M})$
- 6: Construct a rational approximation $r(z) \approx e^z$ on \mathcal{R} such that

$$\max_{z \in \mathcal{R}} |r(z) - e^z| \leq \frac{\epsilon}{(1 + \sqrt{2})\kappa(\mathbf{M})^{1/2}}. \quad (12)$$

Output $r(\mathbf{A})\mathbf{b}$ ($\|r(\mathbf{A})\mathbf{b} - e^{\mathbf{A}}\mathbf{b}\|_2 \leq \epsilon\|\mathbf{b}\|_2$)

3 Numerical examples

This section presents numerical results of the proposed framework described in Algorithm 2. The experiments were conducted on a Mac Studio M4 Max equipped with 128 GB of RAM. All algorithms were implemented in Julia 1.12.3, and the source code is available from the corresponding author upon request. Unless otherwise specified, all computations were performed using IEEE double-precision arithmetic.

3.1 Test problems

We consider a two-dimensional advection-diffusion equation on both a square domain and a star-shaped domain, as illustrated in Figure 2. The governing equation is given by

$$\begin{aligned} \frac{\partial u}{\partial t} &= d\Delta u + \mathbf{c}^\top \nabla u && ((x, y) \in \Omega, t > 0), \\ u(t, x, y) &= 0 && ((x, y) \in \partial\Omega), \\ u(0, x, y) &= u_0(x, y) && ((x, y) \in \Omega, t = 0), \end{aligned} \quad (13)$$

where $d \in \{10^{-1}, 10^{-3}\}$, $\mathbf{c} = [1, 1]^\top$. The initial condition for the square domain is

$$u_0(x, y) = \exp\left(-\sinh(70(x - 1/2)^4) - \sinh(70(y - 1/2)^4)\right), \quad (14)$$

and that for the star-shaped domain is

$$u_0(x, y) = \exp\left(-\sinh(70(x/2)^4) - \sinh(70(y/2)^4)\right). \quad (15)$$

We employ the standard Galerkin discretization with the mesh generated by FreeFEM++ [16]. This yields the following system of ordinary differential equations as a semi-discrete scheme:

$$\mathbf{M}\mathbf{u}'(t) = \mathbf{K}\mathbf{u}(t), \quad \mathbf{u}(0) = \mathbf{b}. \quad (16)$$

An exponential integrator requires to compute $e^{\tau\mathbf{M}^{-1}\mathbf{K}}\mathbf{b}$ for a given time step size τ (\mathbf{b} is replaced with another vector as time integration proceeds).

Since our aim is to check the performance of the proposed method, we employ the linear PDE as our toy problems. We note that even for nonlinear PDEs, an exponential integrator requires the computation of the action of the exponential of matrices of the form $e^{\tau\mathbf{M}^{-1}\mathbf{K}}\mathbf{b}$.

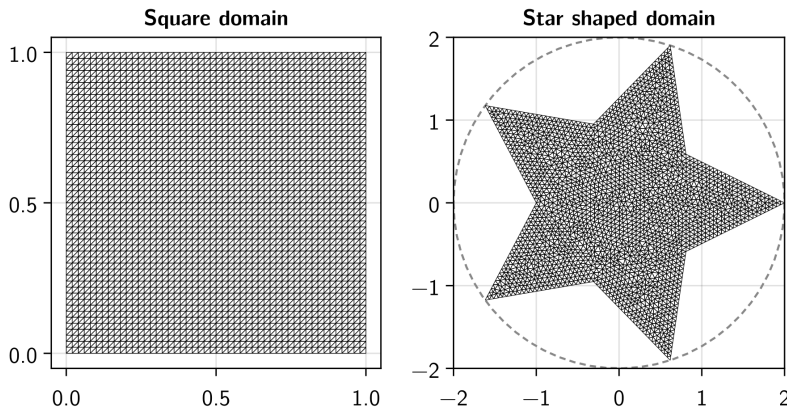


Fig. 2 The square domain and the star-shaped domain we used.

3.2 Computational methods of the matrix exponential

In this test, we consider two computational methods for the matrix exponential.

- **Subdiagonal Padé approximation (sub-pade)**

The Padé approximation of e^z at $z = 0$ has been widely used for computing matrix exponentials and their actions, as its coefficients are available in closed form. Although diagonal [17, 18] or polynomial [3] types are common choice, Güettel et

al. [4] pointed out several advantages of subdiagonal types. For example, the subdiagonal Padé approximation may reduce the computational cost for matrices having large eigenvalues in negative direction, and it can be implemented in partial fraction form. Given the lack of rigorous error estimates for non-symmetric matrices in [4], we employ the following heuristic parameter selection:

- The Padé order is fixed to (4, 5).
- The scaling parameter s_* is chosen to ensure that the approximation error on the rectangle \mathcal{R} is within the target tolerance:

$$s_* = \min \left\{ s = 1, 2, 3, \dots : \sup_{z \in \mathcal{R}} |e^z - (r_{4,5}(z/s))^s| \leq \frac{\epsilon}{(1 + \sqrt{2})\kappa(\mathbf{M})} \right\}, \quad (17)$$

where $r_{4,5}$ is the (4, 5)-type Padé approximant.

- The approximation $r_{4,5}(\mathbf{A}/s) \cdots r_{4,5}(\mathbf{A}/s)\mathbf{b}$ is computed in the partial fraction form, see [4, Sect. 3.2].

- **Rational interpolation (rat-interp)**

Recent advances in algorithms for rational approximation of scalar functions enable the efficient construction of approximations over specified complex domains. Here, we numerically construct a rational approximation in partial fraction form:

$$r_{\text{pf}}(z) = \gamma + \sum_{k=1}^m \frac{\alpha_k}{\beta_k - z} \approx e^z, \quad (18)$$

and evaluate $r_{\text{pf}}(\mathbf{A})\mathbf{b}$. The approximation r_{pf} is constructed by first running the continuum AAA algorithm [19] to determine the poles β_k . Subsequently, the coefficients γ and α_k are determined by solving a linear least-squares problem. Because the coefficient matrix in the linear least square problem can be ill-conditioned, we employ the double-double arithmetic via the `DoubleFloats.jl` package² for solving it.

3.3 Results for checking mathematical validity

Using the medium size matrices, we see several advantages using $\mathcal{W}(\hat{\mathbf{A}})$ rather than $\mathcal{W}(\mathbf{A})$. The advection-diffusion equation (13) is discretized such that the matrix size n is approximately 2000. The time step τ is set to the average mesh edge length \bar{h} . Table 1 summarizes the properties of the test matrices. Their numerical ranges, $\mathcal{W}(\mathbf{A})$ and $\mathcal{W}(\hat{\mathbf{A}})$, are visualized in Figure 3. As shown in Proposition 2, $\mathcal{W}(\hat{\mathbf{A}})$ lies in the left half plane while $\mathcal{W}(\mathbf{A})$ extends into the right half plane.

In the computation, eigenvalues for the pencils $(\tau\mathbf{D}, \mathbf{M})$ and $(\tau\mathbf{C}, \mathbf{M})$ were computed using the `eigvals` function that computes all eigenvalues. The condition number $\kappa(\mathbf{M})$ was obtained via the `cond` function that computes all singular values. Linear systems were solved using a direct solver (`K\b` in Julia). Reference solutions were

²<https://github.com/JuliaMath/DoubleFloats.jl>

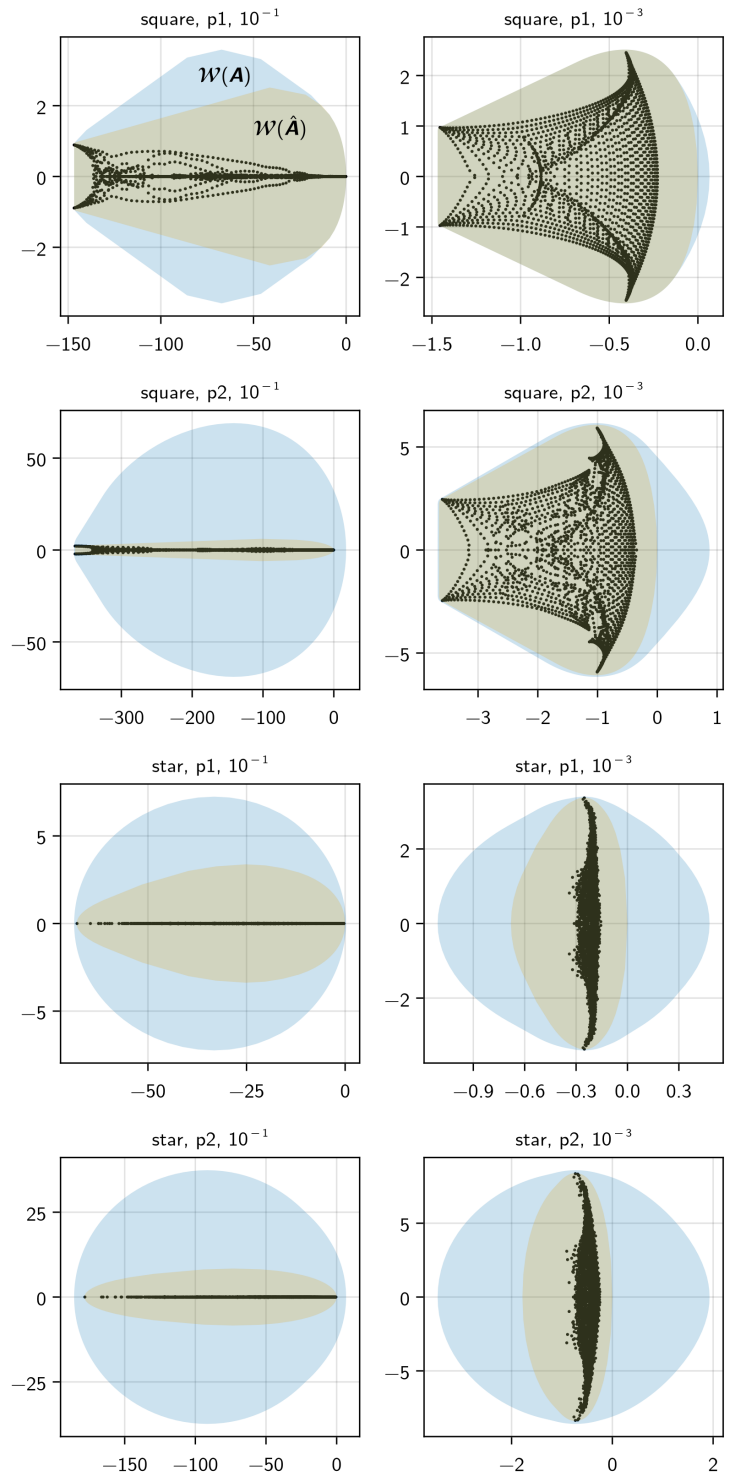


Fig. 3 Eigenvalues and numerical ranges $\mathcal{W}(\mathbf{A})$ and $\mathcal{W}(\hat{\mathbf{A}})$ for the test matrices in Tab. 1. Black dots represent eigenvalues, while blue and orange regions denote $\mathcal{W}(\mathbf{A})$ and $\mathcal{W}(\hat{\mathbf{A}})$, respectively. For these matrices, $\mathcal{W}(\hat{\mathbf{A}})$ is contained within $\mathcal{W}(\mathbf{A})$.

Table 1 Properties of the test matrices $\mathbf{A} = \tau \mathbf{M}^{-1} \mathbf{K}$. Here, n denotes the matrix size and \bar{h} is the average edge length of the mesh.

Shape	Element	d	n	\bar{h}	$\kappa(\mathbf{M})$
square	P1	10^{-1}	2401	2.28×10^{-2}	3.99×10^0
square	P1	10^{-3}	2401	2.28×10^{-2}	3.99×10^0
square	P2	10^{-1}	2401	4.55×10^{-2}	5.81×10^0
square	P2	10^{-3}	2401	4.55×10^{-2}	5.81×10^0
star	P1	10^{-1}	2192	5.51×10^{-2}	6.55×10^0
star	P1	10^{-3}	2192	5.51×10^{-2}	6.55×10^0
star	P2	10^{-1}	2431	1.05×10^{-1}	1.17×10^1
star	P2	10^{-3}	2431	1.05×10^{-1}	1.17×10^1

generated by $\exp(\tau \mathbf{M}^{-1} \mathbf{K}) \mathbf{b}$, where \exp is Julia's built-in function, which is implemented based on the scaling and squaring algorithm in [17]. The target tolerance ϵ was varied from 10^{-8} to 10^{-2} .

Figure 4 shows the approximation errors for each method. Each data point corresponds to a matrix from Table 1. While some cases exhibit overestimation, the error remains below the prescribed tolerance in all instances, confirming that the proposed error control framework functions as intended.

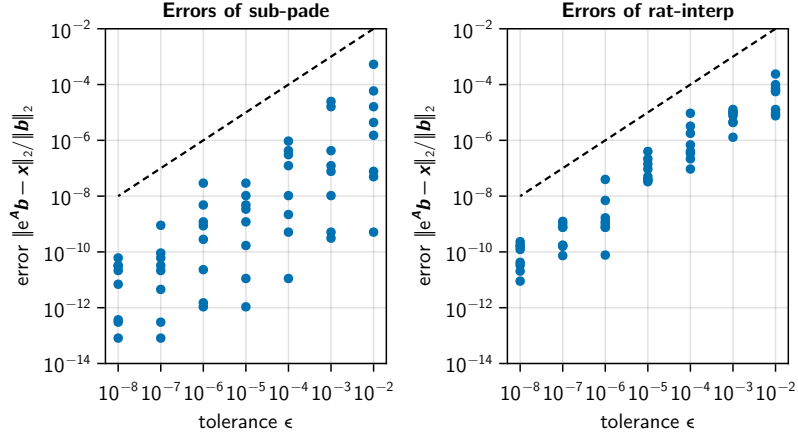


Fig. 4 Errors of each method for $\tau = \bar{h}$. Each point represents the result for one test matrix. Although overestimations occur, the error is smaller than the tolerance for all matrices and methods.

To demonstrate the advantage of using $\mathcal{W}(\hat{\mathbf{A}})$ over $\mathcal{W}(\mathbf{A})$, we compared the complexity of constructing rational functions $r(z)$ with $\epsilon = 10^{-6}$ under two conditions: (i) $|r(z) - e^z| \leq \epsilon/(1 + \sqrt{2})$ on the rectangle enclosing $\mathcal{W}(\mathbf{A})$, and (ii) $|r(z) - e^z| \leq \epsilon/((1 + \sqrt{2})\kappa(\mathbf{M})^{1/2})$ on the rectangle enclosing $\mathcal{W}(\hat{\mathbf{A}})$. Table 2 lists the degrees of the denominators of rational approximations. In all test cases, the degree required for (ii) is less than or equal to that for (i), illustrating the computational advantage gained by using $\mathcal{W}(\hat{\mathbf{A}})$.

Table 2 The degree of the denominator in the rational approximation when $\epsilon = 10^{-6}$. Therefore, smaller numbers are preferable. For **sub-pade**, “—” indicates that the degree exceeded 320 ($s_* > 64$); for **rat-interp**, it indicates a degree exceeding 128.

Shape	Element	d	sub-pade		rat-interp	
			(i) $\mathcal{W}(\mathbf{A})$	(ii) $\mathcal{W}(\hat{\mathbf{A}})$	(i) $\mathcal{W}(\mathbf{A})$	(ii) $\mathcal{W}(\hat{\mathbf{A}})$
square	P1	10^{-1}	25	25	9	9
square	P1	10^{-3}	10	10	5	5
square	P2	10^{-1}	—	25	—	11
square	P2	10^{-3}	25	20	8	8
star	P1	10^{-1}	20	20	11	9
star	P1	10^{-3}	15	15	6	6
star	P2	10^{-1}	185	25	—	12
star	P2	10^{-3}	40	30	10	8

3.4 Results for $e^{\mathbf{A}}\mathbf{b}$ for $\tau = 10\bar{h}$

We further evaluated the framework using a larger time step, $\tau = 10\bar{h}$, with the same matrices \mathbf{M} and \mathbf{K} as in the previous subsection. The resulting errors are shown in Figure 5. With the exception of three cases using **rat-interp** at $\epsilon = 10^{-8}$, the errors consistently fell below the tolerance. In these three cases, the failure occurred during the construction of the partial fraction approximation itself, despite the use of double-double arithmetic. This suggests the limitation lies in the rational approximation step rather than the proposed error control framework.

Table 3 presents the degrees of the denominators for $\tau = 10\bar{h}$. The results indicate that while $\mathcal{W}(\mathbf{A})$ is often too large to construct an accurate rational approximation, $\mathcal{W}(\hat{\mathbf{A}})$ provides a region to construct approximations successfully.

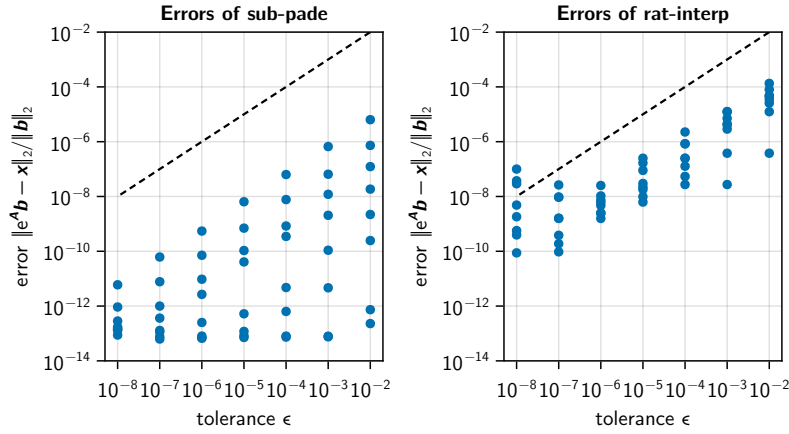


Fig. 5 Approximation errors for $\tau = 10\bar{h}$. Each point represents the result for one test matrix.

Table 3 Denominator degrees for $\epsilon = 10^{-6}$ and $\tau = 10\bar{h}$, following the format of Table 2.

Shape	Element	d	sub-pade		rat-interp	
			(i) $\mathcal{W}(\mathbf{A})$	(ii) $\mathcal{W}(\hat{\mathbf{A}})$	(i) $\mathcal{W}(\mathbf{A})$	(ii) $\mathcal{W}(\hat{\mathbf{A}})$
square	P1	10^{-1}	75	50	22	19
square	P1	10^{-3}	90	85	17	17
square	P2	10^{-1}	–	130	–	31
square	P2	10^{-3}	–	170	–	30
star	P1	10^{-1}	220	75	37	22
star	P1	10^{-3}	200	130	22	19
star	P2	10^{-1}	–	190	–	40
star	P2	10^{-3}	–	310	–	37

3.5 Results for the large matrices

In this section, some results using sparse implementations are presented. The discretization was performed so that the matrix size is approximately 10,000, and τ is set to $5\bar{h}$. Information on the test matrices is listed in Table 4. In the computations, the rectangular region \mathcal{R} and $\kappa(\mathbf{M})$ were computed with `Arpack.jl` package that employs Lanczos method. Here, the Lanczos method was stopped when the relative residual of the Ritz value is 10^{-3} or less. The linear systems were solved using a sparse direct solver provided by `SparseArrays.jl` package. As in previous experiments, the reference solution was computed using Julia’s `exp` function. Figure 6 shows the results. As before, $e^{\mathbf{A}\mathbf{b}}$ was computed with an accuracy corresponding to the error tolerance in all cases.

Table 4 Information on the test matrices $\mathbf{A} = \tau\mathbf{M}^{-1}\mathbf{K}$. Here, n is the size of the matrix, and \bar{h} denotes the average edge length of the mesh.

Shape	Element	d	n	h	$\kappa(\mathbf{M})$
square	P1	10^{-1}	10000	1.13×10^{-2}	4.00×10^0
square	P1	10^{-3}	10000	1.13×10^{-2}	4.00×10^0
square	P2	10^{-1}	10201	2.23×10^{-2}	5.84×10^0
square	P2	10^{-3}	10201	2.23×10^{-2}	5.84×10^0
star	P1	10^{-1}	10504	2.55×10^{-2}	6.98×10^0
star	P1	10^{-3}	10504	2.55×10^{-2}	6.98×10^0
star	P2	10^{-1}	10627	5.08×10^{-2}	1.25×10^1
star	P2	10^{-3}	10627	5.08×10^{-2}	1.25×10^1

4 Conclusion

We proposed an error control framework for computing the matrix exponential of matrices with the structure $\mathbf{A} = \tau\mathbf{M}^{-1}\mathbf{K}$ that relies on $\mathcal{W}(\hat{\mathbf{A}})$ rather than $\mathcal{W}(\mathbf{A})$. The proposed set $\mathcal{W}(\hat{\mathbf{A}})$ is convenient: an enclosing rectangle can be obtained numerically, and if $\mathcal{W}(\mathbf{K})$ lies in the left half plane then $\mathcal{W}(\hat{\mathbf{A}})$ also resides in the left half plane.

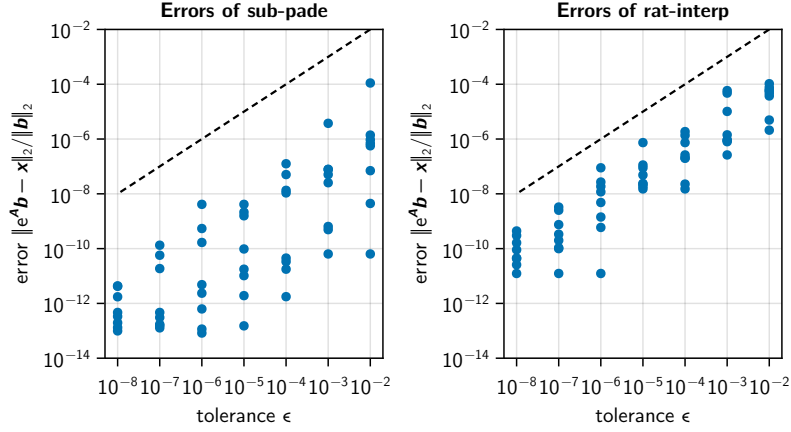


Fig. 6 Approximation errors for matrices in Table 4 with $\tau = 5\bar{h}$. Each point represents the result for one test matrix.

Numerical experiments showed that, once a scalar rational approximation achieving the prescribed accuracy on $\mathcal{W}(\hat{A})$ is obtained, one can compute $e^{\hat{A}}\mathbf{b}$ with an error smaller than or equal to the tolerance.

Future work includes comprehensive performance evaluation in parallel computing environments using large-scale problems.

Declarations

- Funding: this work was partially supported by JSPS KAKENHI grant number 25H00449.
- Conflict of interest: the authors have no relevant financial or non-financial interests to disclose.
- Data/Code availability: the data and the source code are available from the corresponding author upon request.
- Author contribution:
 - F. Tatsuoka: conceptualization, experimentation, writing (original draft).
 - Y. Miyatake: conceptualization, writing (review), supervision
 - T. Sogabe: conceptualization, writing (review), supervision

References

- [1] Higham, N.J.: Functions of Matrices: Theory and Computation. SIAM, Philadelphia, PA (2008). <https://doi.org/10.1137/1.9780898717778>
- [2] Hochbruck, M., Ostermann, A.: Exponential integrators. Acta Numer. **19**, 209–286 (2010) <https://doi.org/10.1017/s0962492910000048>

- [3] Al-Mohy, A.H., Higham, N.J.: Computing the action of the matrix exponential, with an application to exponential integrators. *SIAM J. Sci. Comput.* **33**(2), 488–511 (2011) <https://doi.org/10.1137/100788860>
- [4] Güttel, S., Nakatsukasa, Y.: Scaled and squared subdiagonal Padé approximation for the matrix exponential. *SIAM J. Matrix Anal. Appl.* **37**(1), 145–170 (2016) <https://doi.org/10.1137/15m1027553>
- [5] Caliari, M., Vianello, M., Bergamaschi, L.: Interpolating discrete advection-diffusion propagators at Leja sequences. *J. Comput. Appl. Math.* **172**(1), 79–99 (2004) <https://doi.org/10.1016/j.cam.2003.11.015>
- [6] Caliari, M., Kandolf, P., Ostermann, A., Rainer, S.: The Leja method revisited: backward error analysis for the matrix exponential. *SIAM J. Sci. Comput.* **38**(3), 1639–1661 (2016) <https://doi.org/10.1137/15m1027620>
- [7] Weideman, J.A.C.: Optimizing Talbot’s contours for the inversion of the Laplace transform. *SIAM J. Numer. Anal.* **44**(6), 2342–2362 (2006) <https://doi.org/10.1137/050625837>
- [8] Weideman, J.A.C., Trefethen, L.N.: Parabolic and hyperbolic contours for computing the Bromwich integral. *Math. Comput.* **76**(259), 1341–1357 (2007) <https://doi.org/10.1090/s0025-5718-07-01945-x>
- [9] Tatsuoka, F., Sogabe, T., Kemmochi, T., Zhang, S.-L.: Computing the matrix exponential with the double exponential formula. *Spec. Matrices* **12**(1) (2024) <https://doi.org/10.1515/spma-2024-0013>
- [10] Saad, Y.: Analysis of some Krylov subspace approximations to the matrix exponential operator. *SIAM J. Numer. Anal.* **29**(1), 209–228 (1992) <https://doi.org/10.1137/0729014>
- [11] Gökler, T., Grimm, V.: Convergence analysis of an extended Krylov subspace method for the approximation of operator functions in exponential integrators. *SIAM J. Numer. Anal.* **51**(4), 2189–2213 (2013) <https://doi.org/10.1137/12089226x>
- [12] Güttel, S.: Rational Krylov approximation of matrix functions: numerical methods and optimal pole selection. *GAMM-Mitt.* **36**(1), 8–31 (2013) <https://doi.org/10.1002/gamm.201310002>
- [13] Crouzeix, M., Palencia, C.: The numerical range is a $(1+\sqrt{2})$ -spectral set. *SIAM J. Matrix Anal. Appl.* **38**(2), 649–655 (2017) <https://doi.org/10.1137/17m1116672>
- [14] Johnson, C.R.: Numerical determination of the field of values of a general complex matrix. *SIAM J. Numer. Anal.* **15**(3), 595–602 (1978) <https://doi.org/10.1137/0715039>

- [15] Gökler, T., Grimm, V.: Acceleration of contour integration techniques by rational Krylov subspace methods. *J. Comput. Appl. Math.* **316**, 133–142 (2017) <https://doi.org/10.1016/j.cam.2016.08.040>
- [16] Hecht, F.: New development in FreeFem++. *J. Numer. Math.* **20**(3–4), 251–265 (2012) <https://doi.org/10.1515/jnum-2012-0013>
- [17] Higham, N.J.: The scaling and squaring method for the matrix exponential revisited. *SIAM J. Matrix Anal. Appl.* **26**(4), 1179–1193 (2005) <https://doi.org/10.1137/04061101x>
- [18] Al-Mohy, A.H., Higham, N.J.: A new scaling and squaring algorithm for the matrix exponential. *SIAM J. Matrix Anal. Appl.* **31**(3), 970–989 (2010) <https://doi.org/10.1137/09074721X>
- [19] Driscoll, T.A., Nakatsukasa, Y., Trefethen, L.N.: AAA rational approximation on a continuum. *SIAM J. Sci. Comput.* **46**(2), 929–952 (2024) <https://doi.org/10.1137/23m1570508>